CRYSTAL GROWTH & DESIGN

Article

Controlling size and polymorphism of calcium carbonate hybrid particles using natural biopolymers

Mark Louis P Vidallon, Fiona Yu, and Boon M. Teo

Cryst. Growth Des., **Just Accepted Manuscript** • DOI: 10.1021/acs.cgd.9b01057 • Publication Date (Web): 02 Jan 2020

Just Accepted

is published by the American Chemical Society. 1155 Sixteenth Street N.W., Washington, DC 20036

Controlling size and polymorphism of calcium carbonate hybrid particles using natural biopolymers

*Mark Louis P. Vidallon, Fiona Yu, and Boon M. Teo**

School of Chemistry, Monash University, Clayton, VIC, Australia 3800

ABSTRACT

Calcium carbonate ($CaCO_3$) nanoparticles have diverse applications in biomedicine, including ultrasound imaging, biosensing, drug delivery and theranostics. One of its crystal polymorphs, vaterite, exhibits many unique features, such as its high solubility, porosity and spherical shape, which make it suitable for drug delivery; however, the instability of this polymorph makes the large-scale fabrication of these particles challenging. In this work, we utilized a fast precipitation technique to fabricate $CaCO_3$ hybrid particles, with biocompatible polymeric additives bovine serum albumin (BSA) and polydopamine (PDA), a polymer with unique optical properties. Results showed that BSA and PDA can be used together to produce hybrid particles with variable sizes

and polymorph compositions, depending on the reaction or mixing time applied. We also demonstrated that, by controlling other fabrication process parameters, including the PDA polymerization time, addition order of the salts, and the pairing of the salts with the polymer additives, we could tune the physicochemical properties of the resulting $CaCO_3$ hybrid particles. These findings are important in designing hybrid particle systems with tailored properties for specific applications, including contrast-enhanced ultrasound and photoacoustic imaging, drug delivery, photothermal therapy, and cancer theranostics.

.

Introduction

Calcium carbonate ($CaCO_3$) is one of the most commonly occurring compounds on the Earth's crust. This inorganic compound exhibits ideal properties for drug delivery, such as its biocompatibility,[1] pH responsive nature,[2] porosity, and high encapsulation efficiency.[3] $CaCO_3$ particles can be highly porous, allowing them to efficiently encapsulate therapeutics, and can generate carbon dioxide (CO_2) bubbles in an acidic environment, such as in tumor cells, where the microenvironment pH is approximately 5.5.[4] These properties make $CaCO_3$ particles ideal agents for contrast-enhanced ultrasound imaging and the simultaneous release of therapeutics to tumor sites.[5] $CaCO_3$ has three anhydrous crystal polymorphs – vaterite, calcite and aragonite – that arise from amorphous $CaCO_3$ (ACC).[6-8] These polymorphs have varying properties in terms of their solubility, thermodynamic stability, shape and mean crystal size.[9] Amongst these three polymorphs, vaterite has the highest solubility, dispersion and specific surface area.[10] However, despite these appealing features of vaterite, it has the lowest thermodynamic stability compared to the other two, whereas calcite is the most stable.[10] Although calcite is the most thermodynamically stable polymorph, the stability of the polymorphs largely depends on the presence and properties of additives and their solubility in solution.[11]

Previous research works suggest the application of a versatile, biocompatible polymer, polydopamine (PDA), for controlling the growth of vaterite particles.[8, 12] PDA deposits onto virtually any type and shape of surface via the oxidative self-polymerization of dopamine at slightly basic pH.[13] It became one of the most powerful tools for surface modification[14] and functionalization to develop materials with broad applications in a range of different fields, including biomedical science, energy generation and water treatment.[15] In particular, PDA has been shown to possess an adhesive property, allowing it to influence cell division[16] and reduce the toxicity of encapsulated materials.[17] When applied as coating for particles and surfaces, PDA can suppress the interactions of the coated materials with their surroundings. Moreover, PDA is a major pigment of eumelanin, a compound which has a broad absorption ranging from the visible region to the ultraviolet region in the electromagnetic spectrum[18] in which most of the absorbed photon energy is converted to non-radiative heat.[19] Such optical property of PDA enables it to have wide biomedical applications, including photoacoustic imaging, a technique that utilizes materials that have the ability to generate acoustic waves by absorbing electromagnetic energy.[20] In addition to imaging, PDA has applications in cancer treatment using photothermal therapy.[21-22] This is a minimally invasive technique that uses heat, converted from photon energy, to destroy cancerous cells[23]. Furthermore, several studies have shown that addition of biomacromolecules as additives, such as bovine serum albumin (BSA), in the synthesis of $CaCO_3$ crystals favors the formation of vaterite over the stable polymorph, calcite.[24-26]

To the best of our knowledge, the precise control of the vaterite polymorph of $CaCO_3$ into a sub-micron-sized particle together with PDA and BSA has not been investigated. Herein, we employ a fast precipitation method with solutions containing $CaCl_2$ and Na_2CO_3 and study the influence of various fabrication process parameters (stirring time, polymerization time,

addition order, and salt-polymer pairing) on formation of the $CaCO_3$ hybrid nanoparticles, containing PDA and BSA.

Experiment details

Materials

Calcium chloride dihydrate ($CaCl_2{\cdot}2H_2O$, ≥ 99.0%, Merck), sodium carbonate monohydrate ($Na_2CO_3{\cdot}H_2O$, ≥ 99.5%, Sigma-Aldrich), bovine serum albumin (BSA, ≥ 96%, Sigma-Aldrich), dopamine hydrochloride ($C_8H_{11}NO_7$ HCl, Sigma-Aldrich), and tris(hydroxymethyl)-aminomethane hydrochloride (TRIS HCl, ultrapure, VWR Life Science).

Synthesis of hybrid nanoparticles

Hybrid particles were fabricated using a combination of methods, based on the reports of Mallampati and Valiyaveettil,[27] and Kim and Park.[8] Solutions of $CaCl_2.2H_2O$

and $Na_2CO_3.H_2O$ with concentrations of 33.0 mmol L^{-1} were prepared using 10.0 mmol L^{-1} Tris buffer solution (pH 8.5) as the solvent. Dopamine hydrochloride (DA) and BSA were added to these solutions, depending on the salt-biopolymer pairing shown in Table 1, to achieve concentrations of 4.0 and 9.0 mg mL^{-1}, respectively, which are based on previous optimizations (Figure S1, Supporting Information). The solution, containing DA, was magnetically stirred to initiate polymerization of the monomer into PDA. The two solutions were then combined and magnetically stirred at room temperature to produce the $CaCO_3$ hybrid particles, as a grey-brown to black dispersion. Polymer-salt pairings, addition order, dopamine polymerization times, and $CaCO_3$ stirring times used in all of the experiments are summarized in Table 1. The dispersion was concentrated by centrifugation at 3 400 ×*g* for one minute and washed sequentially with water, ethanol and acetone, prior to drying. The resulting grey powder was stored at 4 °C until further use.

Table 1. Experimental conditions for the fabrication of PDA/BSA/$CaCO_3$ hybrid particles.

Experiment code/name	Dopamine polymerization time (min)*	Stirring time (min)	Polymer-salt pairing	Sequence of addition**

Control	10	3	Only $CaCl_2$ and $NaCO_3$	I
BSA only	10	3	BSA/$CaCl_2$ and $NaCO_3$	I
PDA only	10	3	$CaCl_2$ and PDA/$NaCO_3$	I
Method A	10	2, 3, 4, 10	BSA/$CaCl_2$ and PDA/Na_2CO_3	I
Method B	10	2, 3, 4, 10	BSA/$CaCl_2$ and PDA/Na_2CO_3	II
Method C	10	2, 3, 4, 10	BSA/$NaCO_3$ and PDA/$CaCl_2$	I
Method D	10, 30, 60, 90, 120	3, 4	BSA/$CaCl_2$ and PDA/Na_2CO_3	I

*Dopamine polymerization time refers to the mixing of DA, prior to the combination of salts. During the combination (stirring time) of salts, DA continues to polymerize.

**I - Na_2CO_3 solution added into the $CaCl_2$ solution; II - $CaCl_2$ solution added into the Na_2CO_3 solution.

Characterization

Hydrodynamic diameters and zeta potentials of the particles were determined using dynamic light scattering (DLS) and phase analysis light scattering (PALS), respectively, using a Brookhaven NanoBrook Omni particle sizer and zeta potential analyzer. $CaCO_3$ polymorphs present in the particles were identified using their X-ray diffractograms, obtained with a Bruker D8 Advance Eco X-ray powder diffractometer.

Particle size and morphology of PDA/BSA/$CaCO_3$ hybrid particles were studied using transmission electron microscopy (FEI Tecnai T20 TEM). Samples were prepared by drop casting 3.0 μL dispersions of the particles onto holey carbon film-coated, 300 mesh copper grids (EM Solutions), which were then air-dried prior to imaging.

Results and Discussion

Effect of additives

The synthesis of $CaCO_3$ crystals generally follows one of two methods: the slow CO_2 diffusion method and the fast precipitation method that occurs between dissolved solutions containing Ca^{2+} ions and CO_3^{2-} ions.[28] In the latter method, $CaCO_3$ is produced instantaneously, which poses as a more time favorable technique and therefore more relevant for large-scale productions; however, size control can be very difficult to achieve using this method. Reports in literature suggest that the use of polymer additives can be used to address this problem, as these molecules can establish some interactions with the particles or their precursors, which can control or influence and stabilize their size and crystalline phases.[8, 11, 29-30] In this work, we explored the use of both PDA and BSA in fabricating $CaCO_3$ hybrid particles. Figure 1A shows the schematic representation of the fast precipitation method employed.

TEM images in Figures 1B-1E show the morphologies and polymorphs of the $CaCO_3$ particles produced using the first four methods in Table 1. In the absence of additives (control experiment), the particles produced were a mixture of vaterite and calcite microparticles. Production of porous vaterite microparticles has been reported in a previous work that employed a similar precipitation method with the same salt concentration.[31] For biomedical applications, a porous, sub-micron delivery vehicle, in which active materials such as drugs can be loaded, is ideal; hence, we aimed to control the size, polymorph and morphology of the particles. Upon incorporation of BSA as a stabilizer/additive, sub-micron particles composed of purely vaterite were obtained. In addition to size and polymorph control, we also aimed to confer optical properties to the drug delivery system using PDA to create an interesting design of hybrid particles with multiple capabilities. Similar with using BSA only as the stabilizer/additive, the reaction mixture with PDA yielded only the vaterite polymorph. These results indicate the stabilizing effect that BSA and PDA individually have on vaterite, preventing it from transitioning to the calcite phase. However, highly polydispersed particles were obtained when PDA was used as the additive, compared when BSA was utilized as the polymer additive. Interestingly, when both additives

were utilized in the fabrication of the hybrid particles, particles with a narrow size distribution (PDI = 0.253) with a mean diameter around 572 nm, comprised of both vaterite and calcite, were obtained. The presence of BSA in the hybrid particles was confirmed by SDS-PAGE in Figure S2 (Supporting Information), while the presence of PDA was confirmed by multiple methods including Fourier transform infrared (FTIR) and UV-visible absorption spectroscopy, and TEM, shown in Figures S3-S5 and Table S1 (Supporting Information).

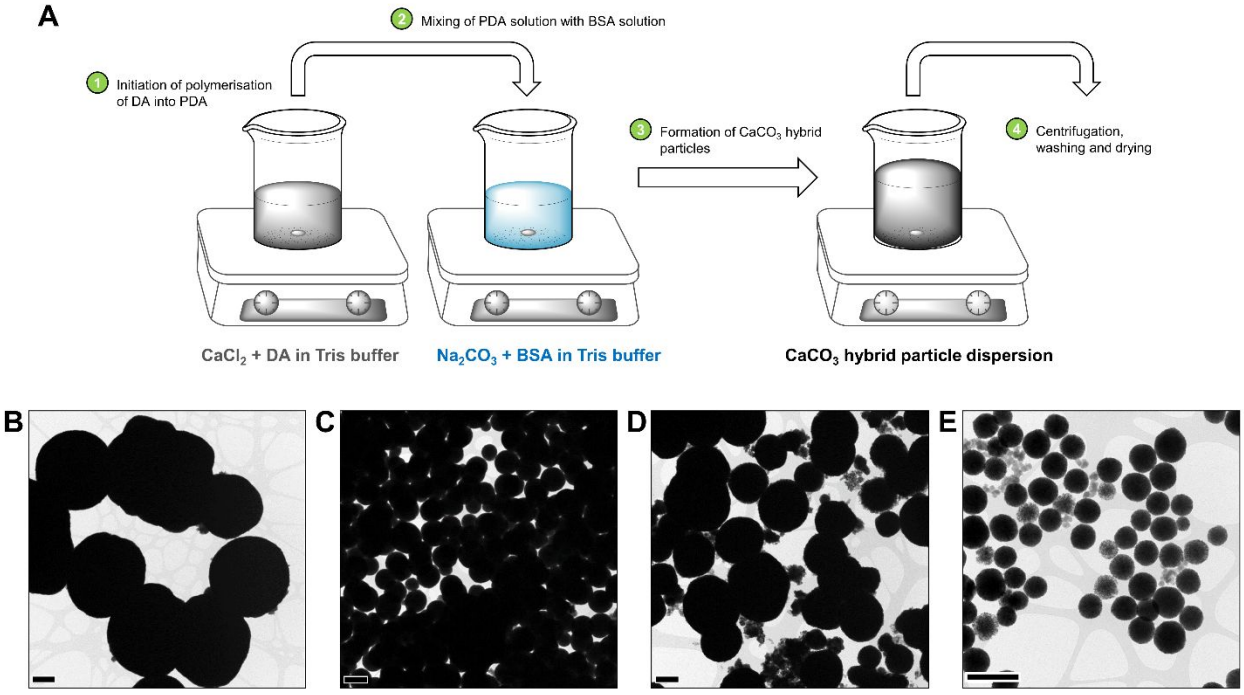

Figure 1. A schematic representation of the experimental method for fabricating PDA/BSA/$CaCO_3$ hybrid particles (**A**). The polymer-salt pairings and addition order shown is for method A and were varied in other parts of the experiment (See details

in Table 1). TEM images of $CaCO_3$ particles obtained in the (**B**) control experiment, with (**C**) BSA only as additive, (**D**) PDA only as additive, and (**E**) method A, with stirring time = 3 minutes. Scale bar = 500 nm.

Vaterite is the most soluble and unstable polymorph of $CaCO_3$ and in the absence of additives, vaterite dissolves easily and recrystallize to form calcite. It has been reported previously[32-33] that the catechol groups of the dopamine molecules can interact with Ca^{2+} and, therefore, slow down the interaction between Ca^{2+} and CO_3^{2-}, resulting in a more controlled growth of the vaterite particles and suppressing it from transitioning into calcite. Similarly, the amide and carboxyl groups present in BSA[26, 34] can also interact with Ca^{2+} and produce a similar effect; however, the presence of both additives BSA and PDA gave rise to a mixture of calcite and vaterite particles. This observation suggests that the biopolymers might be interacting with each other – the hydroxyl and amino groups of dopamine (and PDA) and the polar functionalities of BSA (hydroxyl, amino, amide and carboxyl groups) can form strong hydrogen bonding interactions. These attractive forces between the biopolymers may diminish the

capabilities of the molecules to coordinate effectively with Ca^{2+} and lead to a less controlled particle formation.

Effect of stirring time and sequence of addition

Using the experimental parameters of method A as a starting point, we investigated and compared the influence of stirring time and addition mode or sequence addition of components (method B) on the properties of the hybrid particles obtained. Herein, the stirring time refers to the time in which the $CaCl_2$ and Na_2CO_3 solutions are mixed, in addition to the stirring time for the polymerization of DA into PDA.

Based on DLS and PALS analyses, TEM imaging, and powder X-ray diffractometry (Figure 2), method A initially produced a mixture of vaterite and calcite particles and aggregates, which generally decreased in size and in magnitude of zeta potential over time. This observed decrease in size was accompanied by the transformation of the vaterite polymorph into mostly calcite. These observations are consistent with the expected initial formation of unstable vaterite particles, which can dissolve and re-crystallize/transform into calcite particles with longer stirring time.

We found that swapping the order of the two salt solutions to be added into the other had no effect on the polymorphism of the particles produced, as represented in the TEM images and powder X-ray diffractogram in Figure 2. Both addition modes (methods A and B) gave rise to a mixture of vaterite and calcite particles with comparable mean particle sizes; however, PALS data (Figure 2D) shows that, unlike the particles produced using Method A, those that were obtained from Method B showed almost unchanging zeta potentials. This may indicate that Method A favors better deposition of PDA onto the particles' surface over time, compared with Method B, resulting in the observed change in the surface charge distribution. Another interesting difference is that the samples synthesized via method B had higher polydispersity indexes (PDI) than those that were synthesized via method A. This suggests that the addition of the CO_3^{2-}-containing solution to the Ca^{2+}-containing solution (Method A) yielded particles with more uniform size distribution, which can be a consequence of favored PDA deposition.

A similar observation was reported previously by Wang *et al.*[28] The comparatively high PDI can be attributed to the starting pH values of salt solutions: sodium carbonate in the Tris buffer solution had a pH value of 10.41 and calcium chloride in the Tris

buffer solution had a lower pH value at 7.56. This difference in the initial pH levels prior to reaching the equilibrium pH level of the mixture, may influence the number of initial $CaCO_3$ nuclei that forms and grows into larger particles, which can impact uniformity of the particle sizes;[35] however, this concept has not been extensively studied and therefore warrants further research. For the other experiments described in this paper, mixing mode I (Na_2CO_3 solution added into the $CaCl_2$ solution) was applied, as this addition mode yields particles with lower polydispersity indexes.

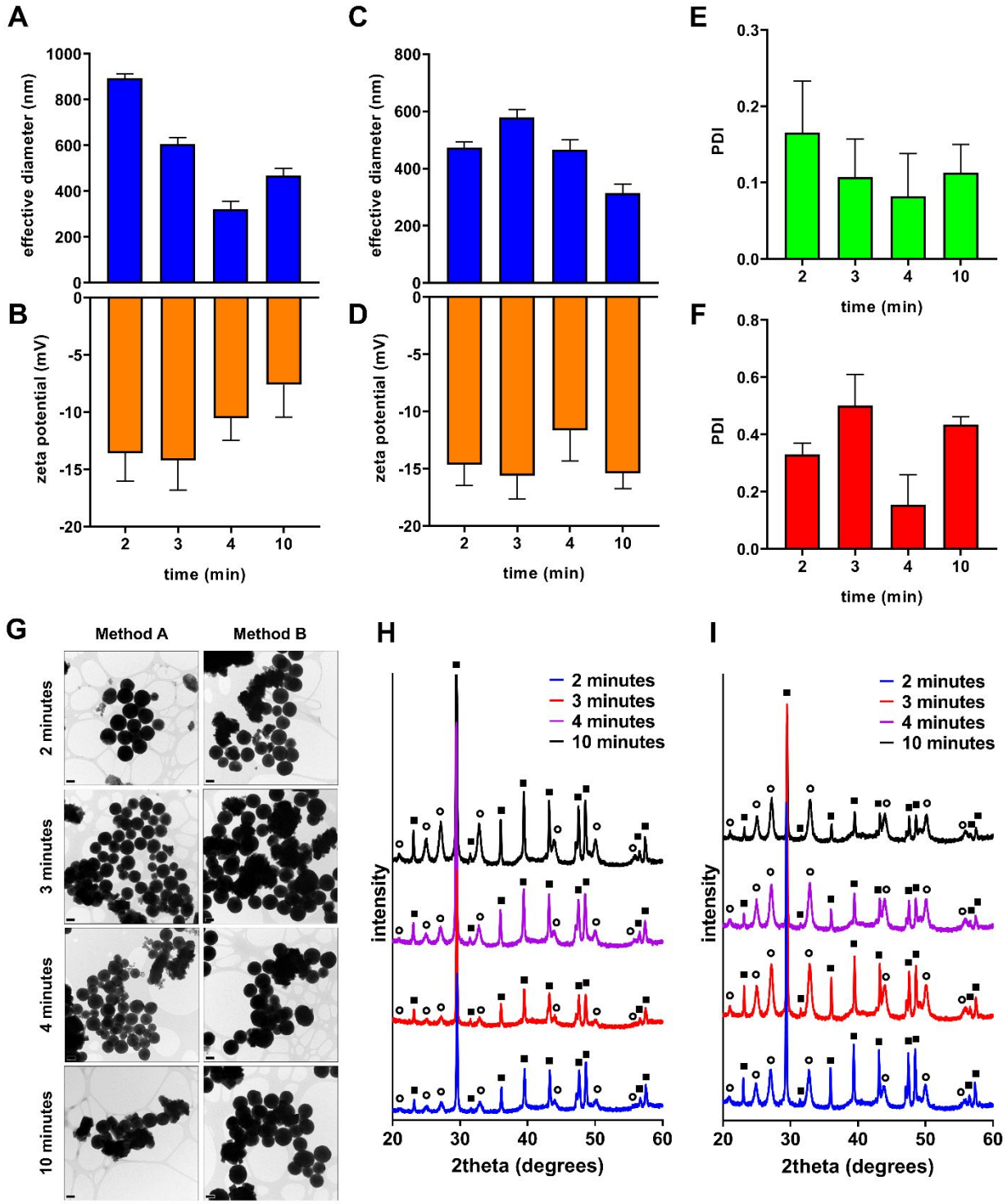

Figure 2. Bar graphs showing the effective diameters, zeta potentials and polydispersity indexes of hybrid particles produced using method A (**A**, **B** and **E**, respectively) and method B (**C**, **D** and **F**, respectively). TEM images (**G**) of hybrid

particles with various stirring times, produced using method A and method B. Scale bar = 500 nm. Powder X-ray diffractograms of particles synthesized via method A (**H**) and method B (**I**) at different reaction times. Squares and circles correspond to calcite (PDF 00-002-0623) and vaterite (PDF 00-060-0483), respectively. Enlarged images of the diffractograms are provided in Figure S6 and S7 (Supporting Information).

Effect of salt-polymer pairing

We also investigated how the pairing of the two polymer additives with $NaCO_3$ and $CaCl_2$ influenced the size, polymorphism, and morphology of the $CaCO_3$ hybrid particles produced. DLS data (Figure 3A) revealed that the hybrid particles obtained from method C are significantly larger, compared to those that were produced using methods A and B. PALS analysis (Figure 3B) showed that the zeta potentials of the particles obtained from Method C are slightly decreasing over time, indicating changes in the surface charge distribution densities of the particles, which may be due to the deposition of PDA. The PDI of the obtained particles, ranging from around 0.1 to 0.3, revealed no general trend (Figure 3C). Interestingly, unlike methods A and B that produced both calcite and vaterite particles, method C almost only produced the

calcite polymorph at all stirring times, as shown by the TEM images (Figures 3D) and powder X-ray diffractograms (Figure 3E). This observed dominant polymorph and the nearly unchanged mean hydrodynamic diameters of the particles obtained at different time points indicate that stable calcite particles are already existent, even at the early stages of the fabrication process.

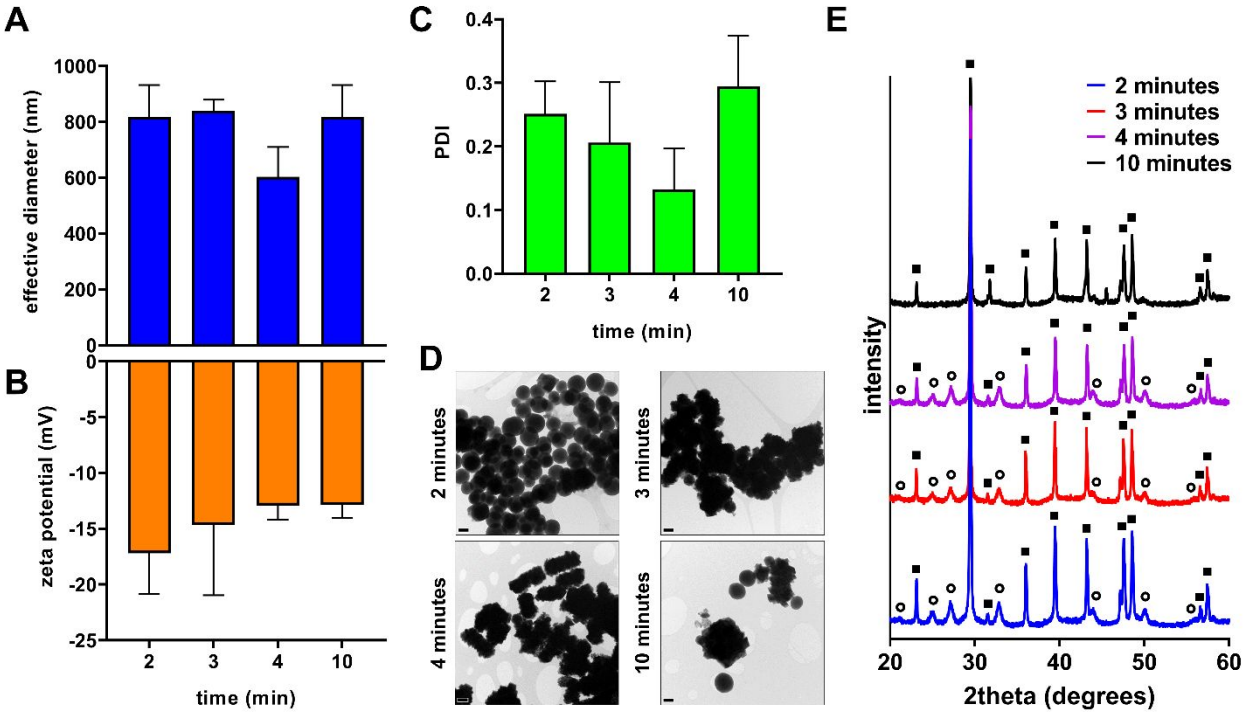

Figure 3. Bar graphs showing the effective diameters (**A**) and zeta potentials (**B**) and polydispersity index (**C**) of hybrid particles produced using method C at different stirring times. TEM images (**D**) of hybrid particles with various stirring times, produced using method C (Scale bar = 500 nm), and their corresponding powder X-ray diffractograms (**E**). Squares and circles correspond to calcite (PDF 00-002-0623) and

vaterite (PDF 00-060-0483), respectively. Enlarged images of the diffractograms are provided in the Figure S8 (Supporting Information).

The differences in the observed polymorphs from methods A and C are mainly due to the interactions of the additives with the Ca^{2+} and CO_3^{2-} ions. It has been reported that Ca^{2+} ions interact with the catechol groups present in dopamine,[32-33] and therefore as dopamine continues to polymerize, free hydroxyl groups are consumed in the reaction, resulting in the depletion of the Ca^{2+}-catecholate complexes.[8, 15] Furthermore, BSA has an overall negative surface charge in basic conditions[36] and no specific interactions with CO_3^{2-}. During the mixing process, it would take time for BSA to combine completely into the mixture and interact effectively with Ca^{2+}. In this case, BSA would be ineffective in slowing down the approach of and reducing the interactions between Ca^{2+} and CO_3^{2-} ions, and in controlling the dissolution and/or re-crystallization of the $CaCO_3$ particles.

In contrast, Method A allows the side chain functional groups present in BSA to coordinate effectively with Ca^{2+}, trapping the ion in a soluble complex.[26] Unlike the interactions between dopamine and Ca^{2+}, the interactions of BSA with Ca^{2+} do not

diminish with increasing stirring time, leading to the controlled nucleation and growth of $CaCO_3$ particles. Moreover, the interaction of both PDA and BSA with the resulting particles limit the dissolution and transformation to the calcite polymorph.

Effect of polymerization time

DLS (Figure 4A) and PALS analyses (Figure 4B) showed no general relationship between the effective diameters and zeta potentials of particles obtained after three minutes of stirring, and the PDA polymerization times used in the study. However, after four minutes of stirring, observed particle sizes tend to increase with increasing polymerization time up to 60 minutes, which then slowly decrease in size from 90 to 120 minutes (Figure 4C). Meanwhile, PALS analysis (Figure 4D) revealed that increasing polymerization time correlates with a decrease in the magnitude of the zeta potential, signifying that the surfaces of the hybrid particles exhibit differences in charge distribution densities, which might be due to the degree of polymerization of the PDA coating. Observed PDI of the particles produced with 3 minutes (Figure 4E) stirring ranged from 0.1 to 0.4, while the PDI of those that were produced with 4

minutes (Figure 4F) stirring ranged from 0.2 to 0.3 with a generally increasing trend with respect to increase in polymerization time.

Shorter polymerization times (10 and 30 minutes), regardless of the stirring time during the mixing of the salt solutions, favors the formation of both vaterite and calcite, while longer polymerization times (60, 90 and 120 minutes) favors the formation of only the calcite polymorph, based on the powder X-ray diffractograms (Figure 4H and 4I). This is supported by the differences in the observed morphologies of the hybrid particles, as shown in the TEM images (Figure 4G). Both 10 and 30 minutes polymerization time yielded a mixture of spherical vaterite particles and more crystalline calcite particles, with evidences of PDA adhesion/incorporation, based on the irregular, low-density materials on the surface of the particles. Starting at 60 minutes to 120 minutes polymerization time, almost no vaterite spheres are observable and large chunks of calcite with PDA coating can be observed. The XRD profiles congruently show the disappearance of the peaks, corresponding to vaterite, with increasing polymerization time. It is also notable that discrete PDA nanoparticles and films formed at 120 minutes polymerization time, which can explain the observed

decrease in the zeta potential with longer polymerization time and at four minutes of stirring after mixing of the salts.

The results suggest that between 30 and 60 minutes, PDA stops becoming effective in suppressing the growth rate of vaterite particles and the transformation of vaterite into calcite takes place. The presence of mainly calcite at longer polymerization times can be attributed to the extensive polymerization into PDA nanoparticles and films (Figure S9, Supporting Information), resulting in the depletion of available dopamine molecules. This leads to a less controlled growth of $CaCO_3$ particles as the calcium-catecholate complex formation is limited and its contribution to the particle stabilization becomes negligible after long polymerization times. Kim and Park[8] reported a similar phenomenon, the preferential formation of calcite microparticles over vaterite spheres, when a dopamine mixture that has been polymerized for 48 hours was utilized to generate the $CaCO_3$ particles.

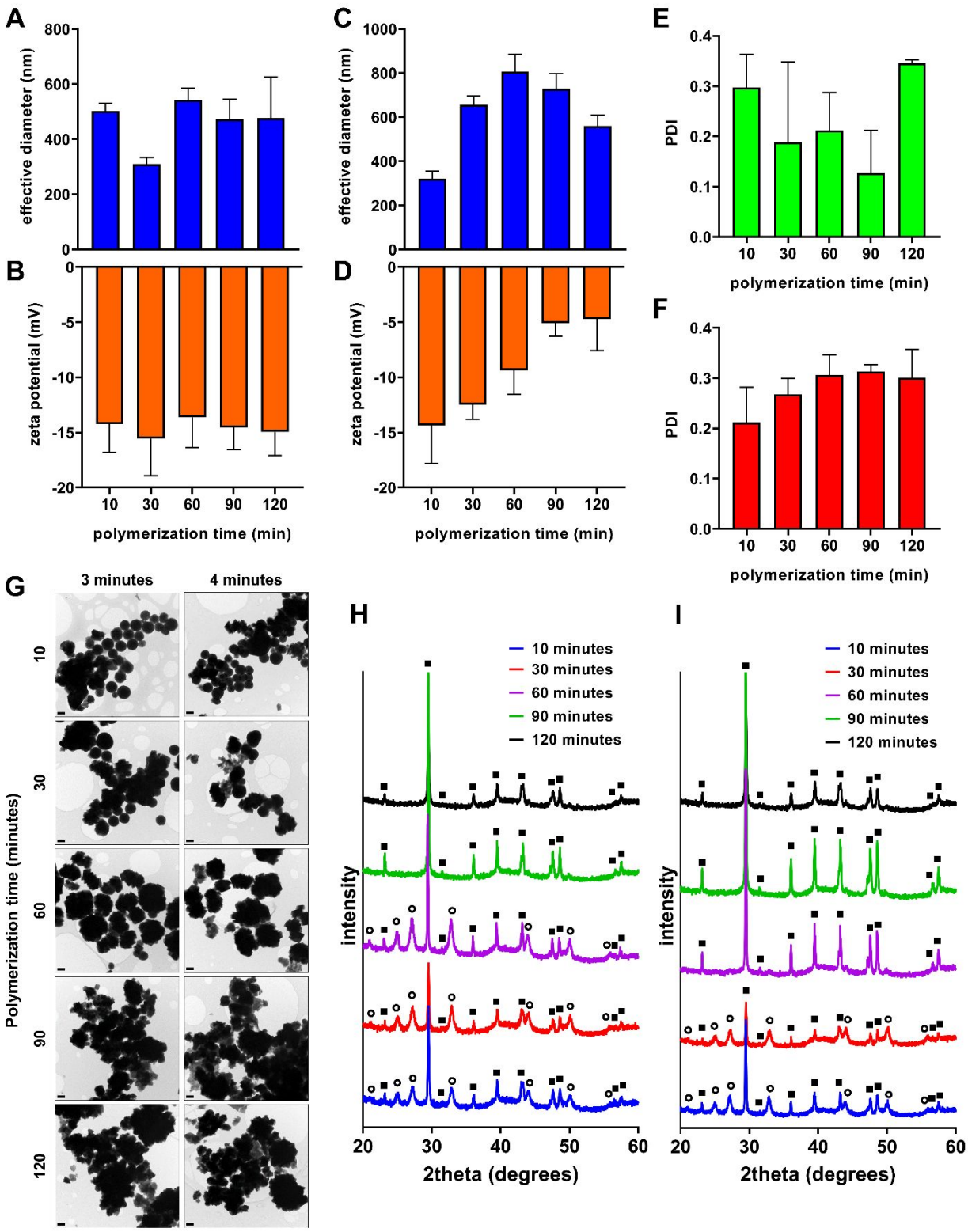

Figure 4. Bar graphs showing the effective diameters and zeta potentials of hybrid particles produced using method D at stirring time = 3 minutes (**A** and **B**, respectively)

and stirring time = 4 minutes (**C** and **D**, respectively) with different PDA polymerization times. TEM images (**G**) of hybrid particles with different polydopamine polymerization times, produced using method D at 3 and 4 minutes stirring time. Scale bar = 500 nm. Powder X-ray diffractograms of particles synthesized via method D at 3 minutes (**H**) and 4 minutes (**I**) stirring time. Squares and circles correspond to calcite (PDF 00-002-0623) and vaterite (PDF 00-060-0483), respectively. Enlarged images of the diffractograms are provided in Figures S10 and S11 (Supporting Information).

Conclusions

In this study, $CaCO_3$ hybrid particles were fabricated via a fast precipitation method using two biocompatible polymers, PDA and BSA. Our work showed that utilizing these additives yields a mixture of vaterite and calcite, which may have particle sizes ranging from around 200 nm to a micron. Manipulating the fabrication process parameters (stirring time, polymerization time, addition order, and salt-polymer pairing) plays a significant role in modifying particle sizes, polymorphs, and morphologies of the resulting particles. Longer stirring times during the precipitation of

the particles allowed the transformation of vaterite into calcite particles. Furthermore, the addition order and salt-polymer pairing were shown to have some effects on the stability of the initially formed vaterite particles and their polydispersity indexes. Stable, submicron-sized, vaterite particles were formed when the BSA/$CaCl_2$ and PDA/Na_2CO_3 pairings were used, with addition of the latter solution the former (addition mode I). Lastly, it was found that PDA loses its ability to control the particle size and influence $CaCO_3$ polymorphism after 30 minutes of polymerization, prior to the precipitation reaction. It was observed that longer polymerization times yielded PDA nanoparticles and films that have limited interactions with the $CaCO_3$ particles, which favored the formation of calcite over the vaterite polymorph. Taken together, we demonstrated that the physicochemical properties of $CaCO_3$ hybrid particles can be precisely tuned by varying a range of parameters. This allows us to design and develop new $CaCO_3$-based materials that can be tailored to specific technologies particularly in drug delivery, sensing, photoacoustic imaging and photothermal therapy.

ASSOCIATED CONTENT

Supporting Information

Powder X-ray diffractograms and optical microscopy images of $CaCO_3$ hybrid particles with different additives, characterisation of PDA/BSA/$CaCO_3$ hybrid particles, and powder X-ray diffractograms with Miller indices of particles from Methods A-D. This material is available free of charge via the Internet at http://pubs.acs.org.

ACKNOWLEDGMENT

The authors acknowledge use of facilities within the Monash Centre for Electron Microscopy and Monash X-ray Platform. The support from Assoc. Prof Rico F. Tabor (School of Chemistry, Monash University) is gratefully acknowledged.

AUTHOR INFORMATION

Corresponding Author

*Correspondence to: Boon M. Teo (boonmian.teo@monash.edu)

Author Contributions

All of the authors contributed equally.

REFERENCES

1. Sukhorukov, G. B.; Volodkin, D. V.; Günther, A. M.; Petrov, A. I.; Shenoy, D. B.; Möhwald, H., Porous Calcium Carbonate Microparticles as Templates for Encapsulation of Bioactive Compounds. *J. Mater. Chem.* **2004**, *14*, 2073-2081.

2. Begum, G.; Reddy, T. N.; Kumar, K. P.; Dhevendar, K.; Singh, S.; Amarnath, M.; Misra, S.; Rangari, V. K.; Rana, R. K., In Situ Strategy to Encapsulate Antibiotics in a Bioinspired CaCO3 Structure Enabling pH-Sensitive Drug Release Apt for Therapeutic and Imaging Applications. *ACS Appl. Mater. Interfaces* **2016**, *8*, 22056-22063.

3. Neira-Carrillo, A.; Yslas, E.; Marini, Y. A.; Vásquez-Quitral, P.; Sánchez, M.; Riveros, A.; Yáñez, D.; Cavallo, P.; Kogan, M. J.; Acevedo, D., Hybrid Biomaterials Based on Calcium Carbonate and Polyaniline Nanoparticles for Application in Photothermal Therapy. *Colloids Surf. B Biointerfaces* **2016**, *145*, 634-642.

4. Gerweck, L. E.; Seetharaman, K., Cellular pH Gradient in Tumor Versus Normal Tissue: Potential Exploitation for the Treatment of Cancer. *Cancer Res.* **1996**, *56*, 1194-1198.

5. Min, K. H.; Min, H. S.; Lee, H. J.; Park, D. J.; Yhee, J. Y.; Kim, K.; Kwon, I. C.; Jeong, S. Y.; Silvestre, O. F.; Chen, X.; Hwang, Y.-S.; Kim, E.-C.; Lee, S. C., pH-Controlled Gas-Generating Mineralized Nanoparticles: A Theranostic Agent for Ultrasound Imaging and Therapy of Cancers. *ACS Nano* **2015**, *9*, 134-145.

6. Rodriguez-Blanco, J. D.; Shaw, S.; Benning, L. G., The kinetics and mechanisms of amorphous calcium carbonate (ACC) crystallization to calcite, viavaterite. *Nanoscale* **2011**, *3*, 265-271.

7. Wang, S.-S.; Xu, A.-W., Amorphous Calcium Carbonate Stabilized by a Flexible Biomimetic Polymer Inspired by Marine Mussels. *Cryst. Growth Des.* **2013**, *13*, 1937-1942.

8. Kim, S.; Park, C. B., Dopamine-induced mineralization of calcium carbonate vaterite microspheres. *Langmuir* **2010**, *26*, 14730-14736.

9. Ševčík, R.; Šašek, P.; Viani, A., Physical and nanomechanical properties of the synthetic anhydrous crystalline CaCO3 polymorphs: vaterite, aragonite and calcite. *J. Mater. Sci.* **2018**, *53*, 4022-4033.

10. Naka, K.; Tanaka, Y.; Chujo, Y., Effect of Anionic Starburst Dendrimers on the Crystallization of CaCO3 in Aqueous Solution: Size Control of Spherical Vaterite Particles. *Langmuir* **2002**, *18*, 3655-3658.

11. Saraya, M. E.-S. I.; Rokbaa, H. H. A. E.-L., Formation and Stabilization of Vaterite Calcium Carbonate by Using Natural Polysaccharide. *Adv. Nanopart.* **2017**, *6*, 25.

12. Dong, Z.; Feng, L.; Hao, Y.; Chen, M.; Gao, M.; Chao, Y.; Zhao, H.; Zhu, W.; Liu, J.; Liang, C.; Zhang, Q.; Liu, Z., Synthesis of Hollow Biomineralized CaCO3–Polydopamine Nanoparticles for Multimodal Imaging-Guided Cancer Photodynamic Therapy with Reduced Skin Photosensitivity. *J. Am. Chem. Soc.* **2018**, *140*, 2165-2178.

13. Lee, H.; Dellatore, S. M.; Miller, W. M.; Messersmith, P. B., Mussel-Inspired Surface Chemistry for Multifunctional Coatings. *Science* **2007**, *318*, 426-430.

14. Ryu, J. H.; Messersmith, P. B.; Lee, H., Polydopamine Surface Chemistry: A Decade of Discovery. *ACS Appl. Mater. Interfaces* **2018**, *10*, 7523-7540.

15. Liu, Y.; Ai, K.; Lu, L., Polydopamine and Its Derivative Materials: Synthesis and Promising Applications in Energy, Environmental, and Biomedical Fields. *Chem. Rev.* **2014**, *114*, 5057-5115.

16. Yang, S. H.; Kang, S. M.; Lee, K.-B.; Chung, T. D.; Lee, H.; Choi, I. S., Mussel-Inspired Encapsulation and Functionalization of Individual Yeast Cells. *J. Am. Chem. Soc.* **2011**, *133*, 2795-2797.

17. Hong, S.; Kim, K. Y.; Wook, H. J.; Park, S. Y.; Lee, K. D.; Lee, D. Y.; Lee, H., Attenuation of the in vivo toxicity of biomaterials by polydopamine surface modification. *Nanomedicine* **2011**, *6*, 793-801.

18. Simon, J. D., Spectroscopic and Dynamic Studies of the Epidermal Chromophores trans -Urocanic Acid and Eumelanin. *Acc. Chem. Res.* **2000**, *33*, 307-313.

19. Forest, S. E.; Simon, J. D., Wavelength-dependent Photoacoustic Calorimetry Study of Melanin. *Photochem. Photobiol.* **1998**, *68*, 296-298.

20. Singh, P.; Sen, K., Drug delivery of sulphanilamide using modified porous calcium carbonate. *Colloid Polym. Sci.* **2018**, *296*, 1711-1718.

21. Li, Y.; Jiang, C.; Zhang, D.; Wang, Y.; Ren, X.; Ai, K.; Chen, X.; Lu, L., Targeted polydopamine nanoparticles enable photoacoustic imaging guided chemo-photothermal synergistic therapy of tumor. *Acta Biomater.* **2017**, *47*, 124-134.

22. Liu, Y.; Ai, K.; Liu, J.; Deng, M.; He, Y.; Lu, L., Dopamine-Melanin Colloidal Nanospheres: An Efficient Near-Infrared Photothermal Therapeutic Agent for In Vivo Cancer Therapy. *Adv. Mater.* **2013**, *25*, 1353-1359.

23. Ibarra, L. E.; Yslas, E. I.; Molina, M. A.; Rivarola, C. R.; Romanini, S.; Barbero, C. A.; Rivarola, V. A.; Bertuzzi, M. L., Near-infrared mediated tumor destruction by photothermal effect of PANI-Np in vivo. *Laser Phys.* **2013**, *23*, 066004.

24. Feng, J.; Wu, G.; Qing, C., Biomimetic synthesis of hollow calcium carbonate with the existence of the agar matrix and bovine serum albumin. *Mater. Sci. Eng. C* **2016**, *58*, 409-411.

25. Li, W.; Liu, L.; Chen, W.; Yu, L.; Li, W.; Yu, H., Calcium carbonate precipitation and crystal morphology induced by microbial carbonic anhydrase and other biological factors. *Process Biochem.* **2010**, *45*, 1017-1021.

26. Liu, Y.; Chen, Y.; Huang, X.; Wu, G., Biomimetic synthesis of calcium carbonate with different morphologies and polymorphs in the presence of bovine serum albumin and soluble starch. *Mater. Sci. Eng. C* **2017**, *79*, 457-464.

27. Mallampati, R.; Valiyaveettil, S., Co-precipitation with calcium carbonate – a fast and nontoxic method for removal of nanopollutants from water? *RSC Adv.* **2015**, *5*, 11023-11028.

28. Wang, Y.; Moo, Y. X.; Chen, C.; Gunawan, P.; Xu, R., Fast precipitation of uniform CaCO3 nanospheres and their transformation to hollow hydroxyapatite nanospheres. *J. Colloid Interface Sci.* **2010**, *352*, 393-400.

29. Olderøy, M. Ø.; Xie, M.; Strand, B. L.; Draget, K. I.; Sikorski, P.; Andreassen, J.-P., Polymorph Switching in the Calcium Carbonate System by Well-Defined Alginate Oligomers. *Cryst. Growth Des.* **2011**, *11*, 520-529.

30. Saraya, M. E.-S. I.; Rokbaa, H. H. A. L., Preparation of Vaterite Calcium Carbonate in the Form of Spherical Nano-size Particles with the Aid of

Polycarboxylate Superplasticizer as a Capping Agent. *Am. J. Nanomater.* **2016**, *4*, 44-51.

31. Petrov, A. I.; Volodkin, D. V.; Sukhorukov, G. B., Protein—Calcium Carbonate Coprecipitation: A Tool for Protein Encapsulation. *Biotechnol. Progr.* **2005**, *21*, 918-925.

32. Holten-Andersen, N.; Mates, T. E.; Toprak, M. S.; Stucky, G. D.; Zok, F. W.; Waite, J. H., Metals and the Integrity of a Biological Coating: The Cuticle of Mussel Byssus. *Langmuir* **2009**, *25*, 3323-3326.

33. Xu, Z., Mechanics of metal-catecholate complexes: The roles of coordination state and metal types. *Sci. Rep.* **2013**, *3*, 2914.

34. Shemin, D., Amino acid determinations on crystalline bovine and human serum albumin by the isotope dilution method. *J. Biol. Chem.* **1945**, *159*, 439.

35. Boyjoo, Y.; Pareek, V. K.; Liu, J., Synthesis of micro and nano-sized calcium carbonate particles and their applications. *J. Mater. Chem.* **2014**, *2*, 14270-14288.

36. Böhme, U.; Scheler, U., Effective charge of bovine serum albumin determined by electrophoresis NMR. *Chem. Phys. Lett.* **2007**, *435*, 342-345.

For Table of Contents Use Only

Controlling size and polymorphism of calcium carbonate hybrid particles using natural biopolymers

Mark Louis P. Vidallon, Fiona Yu, and Boon M. Teo

Synopsis

Manipulating the size and polymorphism of calcium carbonate particles can be a challenging task. In this work, we utilized two natural biopolymers, polydopamine and bovine serum albumin, and optimized a set of process parameters to fabricate hybrid particles and demonstrate the possibility of tuning their physicochemical properties.